Comparing 433 and 868 MHz active RFID for indoor localization using multi-wall model

Reference:
Berkvens Rafael, Smolders Frederik, Bellekens Ben, Aernouts Michiel, Weyn Maarten.- Comparing 433 and 868 MHz active RFID for indoor localization using multi-w all model
2018 8th International Conference On Localization And GNSS Seamless Indoor-Outdoor Localization, 26-28 June, 2018, Guimarães, Portugal - ISSN 2325-0771 - IEEE, 2018, p. 1-6
Full text (Publisher's DOI): https://doi.org/10.1109/ICL-GNSS.2018.8440905

Comparing 433 and 868 MHz Active RFID for Indoor Localization Using Multi-Wall Model

Rafael Berkvens, Frederik Smolders, Ben Bellekens, Michiel Aernouts, and Maarten Weyn
University of Antwerp - imec
IDLab - Faculty of Applied Engineering
Groenenborgerlaan 171, 2020 Antwerp, Belgium
E-mail: rafael.berkvens@uantwerpen.be

***Abstract*—Active radio frequency identification is a common technology in many logistical applications. Advanced standards, like DASH7, allow more than just identification and bring wireless connectivity to those industries using communication frequencies below 1 GHz. Based on these communication links, we want to enable localization, so that items can be tracked throughout the environment. In this paper, we compare the two European license exempt frequencies for DASH communication, 433 MHz and 868 MHz, as a method for localizing, using a multi-wall propagation model. In an office environment, we find that 433 MHz leads to an average location error of 8.27 m and 868 MHz to 1.27 m. The result for 868 MHz is encouraging for further study of such approaches.**

***Keywords*—Indoor localization, multi-wall propagation model, active RFID**

I. Introduction

Active RFID (Radio Frequency Identification) is an energy efficient, cost effective multi-object recognition technology [1] that is already being used intensively in warehouse management. Developments in the Internet of Things (IoT) [2] show the need for context information, especially location information [3], for various applications. Thus, we want to investigate how to localize devices through the use of the commonly available active RFID communication infrastructure. While sub-GHz frequencies in active RFID do not typically perform well on range estimations through either signal attenuation or time of arrival, this is compensated by the low power consumption of the technology. To increase the localization performance, we will use a multi-wall model of the environment in an attempt to better model the signal attenuation.

Localization by radio communication signals has an advantage over more commonly known satellite localization, such as the Global Positioning System (GPS), because localization by radio communication can operate properly in indoor scenarios. Several techniques for indoor localization by radio communication exist. Guang-yao Jin et al. [4] improve the LANDMARC [5] RFID localization system, which uses a number of reference tags with known locations. Fixed RFID readers can sense both the reference tags and mobile target tags, and can then infer the location of the target tags by comparing the relative signal strengths. They achieve a location error of less than one meter, with reference tags placed in a regular grid of two by two meter cells. LANDMARC operates at 308 MHz [5]. Montaser and Moselhi [6] use RFID in a combination of proximity and signal strength trilateration localization in areas of about 100 m^2, achieving a mean location error of 1 m using between 20 and 30 reference tags. The authors state that they use Ultra High Frequency (UHF) RFID, but do not specify which carrier frequency exactly.

Other radio communication systems that are used for localization include: Bluetooth Low Energy (BLE) [7], ZigBee [8], and Wi-Fi [9, 10, 11], which operate at 2.4 GHz and have a typical location error between 1 m to 10 m; and Ultra Wide Band (UWB) [12], which operates at 3.5 GHz and typically achieves a sub-meter accuracy. UWB localization can be very accurate, yet requires Line Of Sight (LOS) for its high performance, which cannot always be guaranteed. Wi-Fi is commonly used in the form of fingerprinting, which is a useful technology for wireless localization which is quite accurate with a mean error of 6.1 m [11]. However, maintaining a fingerprint database is time and energy consuming, especially in places where objects often change from location to location.

In this paper, we utilize DASH7 as our active RFID protocol. DASH7 is an open source Wireless Sensor and Actuator Network (WSAN) protocol that aims for medium range, low power communication over unlicensed sub-GHz bands specified and promoted by the DASH7 Alliance [13]. It has its roots in the ISO 18000-7 RFID standard. However, DASH7 is capable of more than just RFID. It defines a complete WSAN communication stack, implementing each layer of the Open Systems Interconnection (OSI) model and ensures interoperability amongst different providers. DASH7 operates at 433 MHz and 915 MHz, which are industrial, scientific and medical (ISM) radio bands, and 868 MHz, which is also an unlicensed sub-GHz band. Moreover, it can be used at low, normal or high rate, which is respectively 9.6 kbps, 55.6 kbps, or 166.7 kbps.

Localization using DASH7 has been studied before [14, 15]. However, this paper reports on researcher that goes beyond previous research by comparing the different frequencies at which it operates in Europe, 433 MHz and 868 MHz. Additionally, this paper creates a wall attenuation model specific for each of these frequencies, rather than relying on the 915 MHz model used by [14]. We use the same 1122 m^2 office environment that has been used before, but updated the hardware so that it can operate both on 433 MHz and 868 MHz.

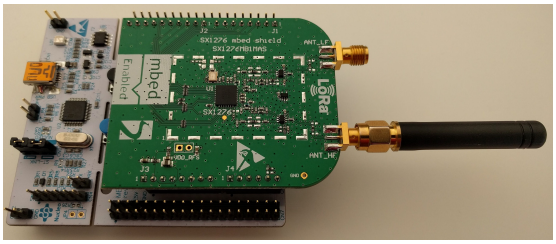

Fig. 1. Both the gateway and the mobile node consist of a SX1276MB1xAS shield attached to a NUCLEO development board; the gateways further consist of a Raspberry Pi 3 model B at which communicated with the development board.

This paper continues as follows. First, Section II describes how the measurements are performed. Next, Section III explains the propagation model and Section IV describes the localization method. Then, Section V provides the results of our experiments. Finally, Section VI gives the conclusion of this paper.

II. Measurements Methodology

Our experiment involves one mobile tag or node and six RFID readers or gateways. The gateways are connected over Ethernet to a central network server. The mobile tag sends messages to the gateways in regular intervals of 100 ms. We perform the experiment twice: once for 433 MHz and once for 868 MHz. When a gateway receives the message, it will report the received signal strength (RSS) to the central network server. The server will then utilize the gateway topology and multi-wall model to calculate a position, which are detailed in Sections III and IV.

We use Nucleo L073RZ development boards from ST Microelectronics, attached to a SX1276MB1xAS radio shield, see Figure 1. The radio shield used the DASH7 protocol [13] in the Open Source Stack version [16]. The mobile node uses only this platform, the gateways are connected to a Raspberry Pi (RPi) single-board computer. The RPi publishes the received signal strength reported by the development board's radio shield to the central network server using MQTT.

In the experiment, we place the mobile node at 25 different locations in the environment. First, the node broadcasts messages every 100 ms at 433.06 MHz center frequency; afterwards, it broadcasts at 863 MHz center frequency. On average, the mobile node sends 304 messages for each frequency at a single location. We did not optimize the gateways' position for either localization or signal reception, but we did try to distribute them evenly through the office environment. The gateways were also first programmed to listen at 433 MHz and afterwards at 868 MHz. The placement of the gateways and the positions of the mobile node is shown in Figure 2, where the gateways are shown with red dots and the positions of the mobile node with green triangles.

III. Propagation Model

When a gateway receives a message from the node, the transmission loss between them can be theoretically estimated.

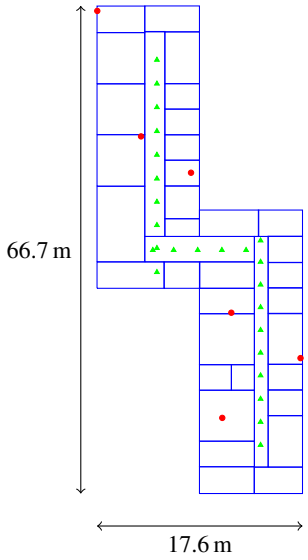

Fig. 2. The test environment setup. The red dots are the locations of the gateways. The green triangles are the locations where the mobile node is placed.

It can be modeled by using a propagation loss model. There are two main types of propagation models [17]. First, there are empirical models which are less complicated but also less accurate, as they provide a statistical solution based on multiple measurements. Second, there are deterministic models which are more complicated. These models are divided into two subcategories: site-general models, which include fading effects caused by walls and ceilings; and site-specific models, which also include small-scale fading effects like reflections and refractions. Site-specific models require a lot more details in order to implement these small-scale fading effects. Due to this, they require more complex calculations.

Our experiment uses a site-general model which considers the loss due to walls and ceilings. The test location has been divided into an equally sized grid with a resolution of 0.3 m. This will enable it to compute the Euclidean distance between each grid cell and the location of the mobile node. This distance allows us to calculate the link budget L according to a modified version of the extended ITU model [18] that has the following equation:

$$L = 20 \log f + 10n \log d + X_a(k) - 28, \qquad (1)$$

where L is the link budget in [dB], f is the frequency in [MHz], d is the Euclidean distance in [m], n is a constant factor to calculate the link budget in LOS over a certain distance, and $X_a(k)$ is the multi internal wall attenuation loss factor in [dB]. Subsequently, the number of wall penetrations is computed by calculating the number of intersections between a line drawn from a specific grid cell to the mobile node's location, with the walls drawn in Figure 2.

The number of wall penetrations k is used as input to determine the wall attenuation path loss X_a according to the

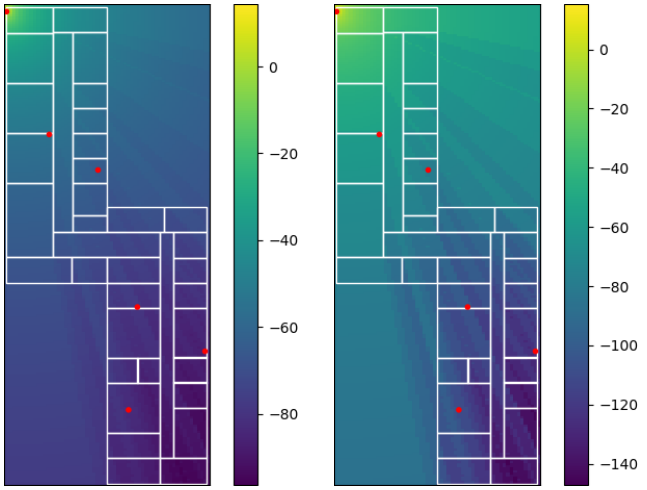

(a) (b)

Fig. 3. The link budgets of the gateway in the upper left corner of the environment are plotted based on the multi-wall propagation model at (a) 433 MHz and (b) 868 MHz.

following formula, which has been determined for both 433 MHz and 868 MHz separately:

$$X_{a,433}(k) = 1.5455k + 1.6768, \tag{2}$$

$$X_{a,868}(k) = 5k. \tag{3}$$

To determine the parameters, we took the median of all the link budgets gathered by sending about 100 messages for both 433 MHz and 868 MHz at a reference distance of exactly one meter. We did the experiment in the same manner for the two frequencies, while a distance of 1.4 m is theoretically optimal for 433 MHz. Subsequently, to determine n in Equation (1), we measured the link budget at certain distances, and fitted a model to these values. About 100 link budgets were measured every two meters, up to 20 m in open field along a straight line for both 433 MHz and 868 MHz. The reference values for one meter were subtracted from those values so that the link budget over a certain distance could be calculated.

Figure 3 shows the results after applying these calculations for each grid cell of the environment for respectively 433 MHz and 868 MHz. They show the signal strength relative to the gateway in the upper left corner.

IV. Localization Method

When a gateway receives a message from the mobile node, it measures the RSS and publishes this to the central server. The server gathers these measurements from all gateways that receive the message. This list of RSS values L^m, the server calculates the probability p the mobile node is at location X. It commences by calculating the likelihood $p(L_n^m \mid X)$ for each RSS value L_n^m of each gateway n at each location in X using a Gaussian noise model and the propagation model in Equation(1):

$$p(L_n^m \mid X) = \frac{1}{\sigma\sqrt{2\pi}} \exp -\frac{1}{2}\left(\frac{L_n^m - L_n}{\sigma}\right)^2, \tag{4}$$

where L_n^m is the link budget measured between the mobile node and the gateway n, L_n is the link budget calculated by the multi-wall propagation model, and σ is experimentally determined by a number of measurements.

To form the joint likelihood distribution, the likelihoods from all the different gateways N in a single link budget measurement L^m are multiplied, making the assumption that the RSS values measured at the different gateways are independent:

$$p(L^m \mid X) = \prod_N^n p(L_n^m \mid X). \tag{5}$$

Subsequently, the posterior probability is calculated by using Bayes' formula with a uniform prior $p(X)$:

$$p(X \mid L^m) = \frac{p(L^m \mid X)p(X)}{\sum_X p(L^m \mid X)}. \tag{6}$$

Finally, the location X with the highest posterior probability is the location at which we estimate that the mobile node is located. When there are multiple locations with this posterior probability, the first of those locations in the grid is selected as a naive implementation choice; there is room for improvement here, although it does not occur frequently. The location error can then be defined as the Euclidean distance between the actual location and the estimated location of the mobile node.

V. Results

The results are twofold. One one hand, we determined the specific parameters of the propagation model, specific for our frequency, hardware, and environment. These parameters are what makes the difference with our previous research. On the other hand, we analyzed the localization results using these parameters.

Figure 4 shows the link budget as measured at a distance of one meter between the mobile node and the gateway. While the setup using 433 MHz results in a constant link budget, using 868 MHz results in some fluctuations. The reference link budget in the ITU model, Equation (1), is chosen to be 33 dB for 433 MHz and 32 dB for 868 MHz.

Figure 5 shows the link budget as measured in line of sight at intervals of 2 m between the mobile node and the gateway, with a maximum distance of 20 m. These values are approximated by a logarithmic function to determine n in the ITU model. The value for 433 MHz is 3.4373, the value for 868 MHz is 3.1528.

Figure 6 shows the functions that are used to calculate the additional attenuation caused by walls intersecting the direct line between the mobile node and the gateway. These functions approximate a set of measurements, which were performed in multiple adjacent rooms. In the first room, we placed the gateway, at at least one meter from any wall. In the second room, we placed the mobile node, again at least one meter away from any wall. As in the localization experiment, the antenna polarizations are the same for mobile node and gateway. The difference between the signal attenuation measured at the gateway and the signal attenuation predicted by the ITU model

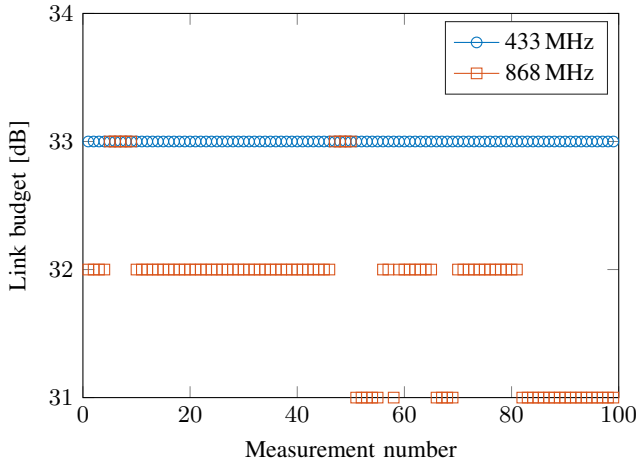

Fig. 4. Link budgets measured at a reference distance of one meter for 433 MHz and 868 MHz.

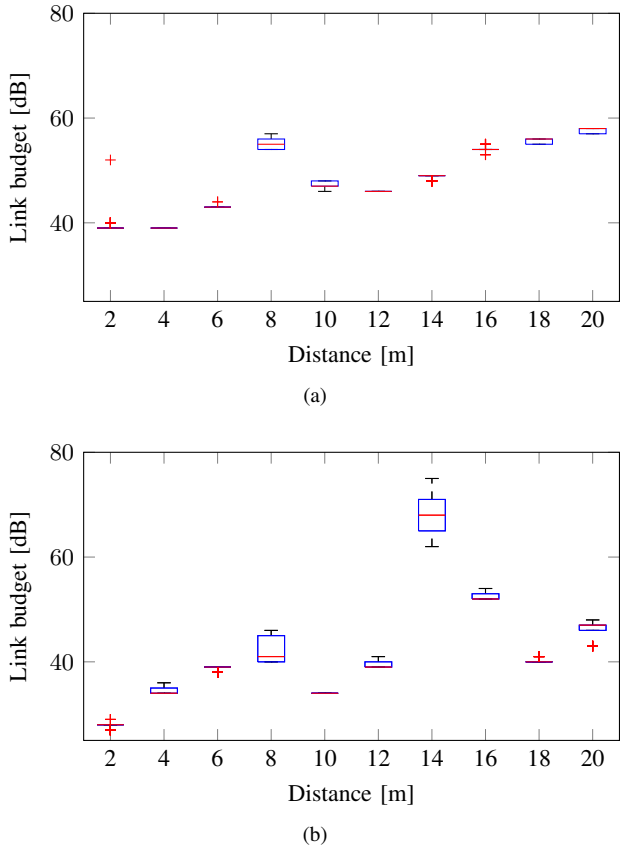

Fig. 5. Boxplots of Line of Sight measurements every two meters for (a) 433 MHz and (b) 868 MHz.

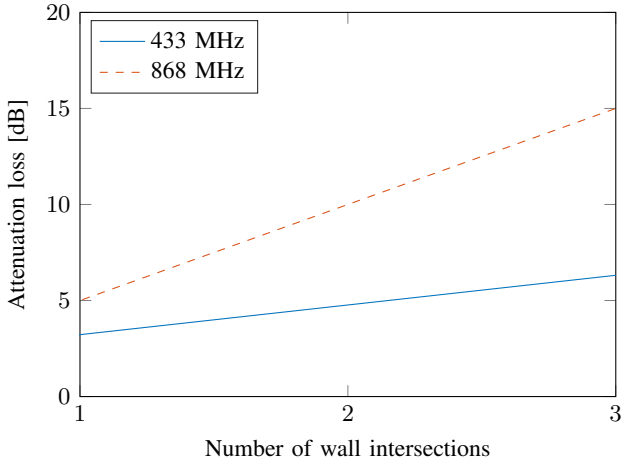

Fig. 6. Atennuation loss caused by walls for 433 MHz and 868 MHz.

TABLE I
KEY FIGURES OF THE LOCALIZATION ERRORS.

	433 MHz [m]	868 MHz [m]
Mean	8.27	1.27
Median	8.24	1.15
Standard deviation	4.26	0.74
75th percentile	10.44	1.62

was counted as the attenuation caused by the wall. Next, the mobile node was replaced to the following adjacent room, so that two walls were between the mobile node and the gateway. The procedure to determine the attenuation caused by one wall was repeated for the two walls, and another time for three walls. The resulting measurements were best approximated by a linear function in the form $y = ax+b$, with y the attenuation and x the number of walls. For 433 MHz, the value of a is 1.5455 and b is 1.6768; for 868 MHz, the value of a is 5 and b is 0.

With the parameters for the ITU model and wall attenuation, we can start localizing the mobile node. Figure 7 shows the true locations and estimated locations for both 433 MHz and 868 MHz. A line connects the true and estimated locations, so that the typical locations of incorrect estimations are clearly visible. Table I summarizes the localization results. For 433 MHz, the mean location error is 8.27 m, with a standard deviation of 4.26 m. This means that on average, the 433 MHz communication setting can only roughly indicate the location of a device. For 868 MHz, however, the mean location error is 1.27 m, with a standard deviation of 0.74 m. This is much smaller than the mean location error reported in [14], 5.3 m, probably because the parameters in the propagation model are now set to values determined by experiments specifically for this frequency. This distinction is further confirmed by the 50th (median) and 75th percentile error: for 433 MHz respectively 8.24 m and 10.44 m; for 868 MHz respectively 1.15 m and 1.62 m.

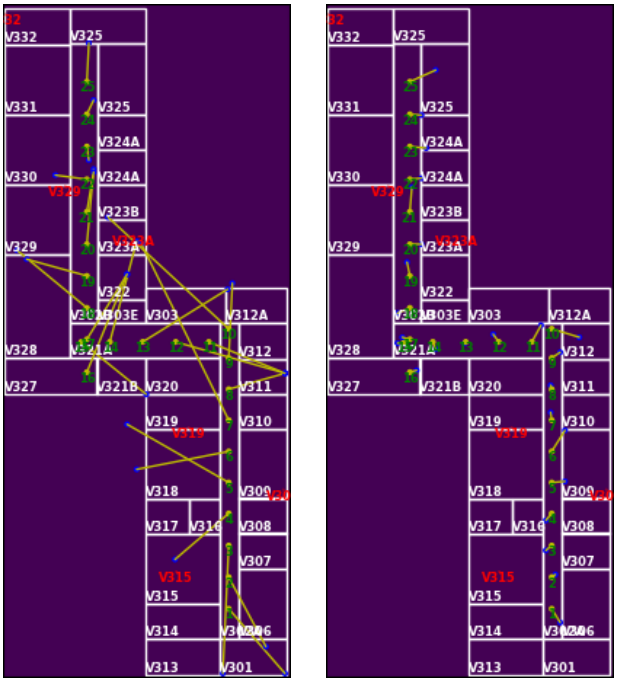

(a) (b)

Fig. 7. The actual locations and the locations measured by the propagation model for (a) 433 MHz and (b) 868 MHz are plotted in yellow and blue respectively.

VI. Conclusion

This paper presents a comparison between the 433 MHz and 868 MHz frequencies for indoor localization using DASH7 communication and a multi-wall propagation model. Our approach results in a mean error of 8.27 m for 433 MHz and 1.27 m for 868 MHz. This is a large improvement over our previous implementation of the multi-wall model for 868 MHz [14]. Since this localization system makes use of the multi-wall propagation model, no fingerprint database has to be maintained.

Our future work includes an improved maximum a posteriori selection. Currently, when two locations have the same posterior probability value, the first location in the grid is selected. This is of course purely arbitrary and could be improved, for example by filtering the location estimates over time. Another point of improvement is the value for sigma in Equation (4). It is save to assume that the variation of the link budget will increase as the distance between gateway and mobile node increases. Finally, we will also compare this site general propagation model to a site specific propagation model based on ray casting [19]. Such a site-specific propagation loss model allows us to incorporate the influences introduced due to small-scale fading effects. This will result in a more realistic likelihood distribution that will lead to a more realistic location estimation.

Acknowledgment

Part of this work was funded by the MuSCLe-IoT (Multimodal Sub-Gigahertz Communication and Localization for Low-power IoT applications) project, co-funded by imec, a research institute founded by the Flemish Government, with project support from VLAIO (contract number HBC.2016.0660). Part of this research was funded by the Flemish FWO SBO S004017N IDEAL-IoT (Intelligent DEnse And Longe range IoT networks) project.

References

[1] D. Zhang, L. T. Yang, M. Chen, S. Zhao, M. Guo, and Y. Zhang, "Real-Time Locating Systems Using Active RFID for Internet of Things," *IEEE Systems Journal*, vol. 10, no. 3, pp. 1226–1235, sep 2016.

[2] L. Atzori, A. Iera, and G. Morabito, "The Internet of Things: A survey," *Computer Networks*, vol. 54, no. 15, pp. 2787–2805, oct 2010.

[3] J. Lin, W. Yu, N. Zhang, X. Yang, H. Zhang, and W. Zhao, "A Survey on Internet of Things: Architecture, Enabling Technologies, Security and Privacy, and Applications," *IEEE Internet of Things Journal*, vol. 4, no. 5, pp. 1125–1142, oct 2017.

[4] Guang-yao Jin, Xiao-yi Lu, and Myong-Soon Park, "An Indoor Localization Mechanism Using Active RFID Tag," in *IEEE International Conference on Sensor Networks, Ubiquitous, and Trustworthy Computing -Vol 1 (SUTC'06)*, vol. 1. Taichung, Taiwan: IEEE, 2006, pp. 40–43.

[5] L. M. Ni, Y. Liu, Y. C. Lau, and A. P. Patil, "LANDMARC: Indoor Location Sensing Using Active RFID," *Wireless Networks*, vol. 10, no. 6, pp. 701–710, nov 2004.

[6] A. Montaser and O. Moselhi, "RFID indoor location identification for construction projects," *Automation in Construction*, vol. 39, pp. 167–179, apr 2014.

[7] H. Li, "Low-Cost 3D Bluetooth Indoor Positioning with Least Square," *Wireless Personal Communications*, vol. 78, no. 2, pp. 1331–1344, sep 2014.

[8] J. V. Marti, J. Sales, R. Marin, and E. Jimenez-Ruiz, "Localization of Mobile Sensors and Actuators for Intervention in Low-Visibility Conditions: The ZigBee Fingerprinting Approach," *International Journal of Distributed Sensor Networks*, vol. 8, no. 8, p. 951213, aug 2012.

[9] J. Torres, O. Belmonte, R. Montoliu, S. Trilles, and A. Calia, "How Feasible Is WiFi Fingerprint-Based Indoor Positioning for In-Home Monitoring?" in *2016 12th International Conference on Intelligent Environments (IE)*. IEEE, sep 2016, pp. 68–75.

[10] A. R. Jimenez Ruiz, F. Seco Granja, J. C. Prieto Honorato, and J. I. Guevara Rosas, "Accurate Pedestrian Indoor Navigation by Tightly Coupling Foot-Mounted IMU and RFID Measurements," *IEEE Transactions on Instrumentation and Measurement*, vol. 61, no. 1, pp. 178–189, jan 2012.

[11] J. Torres-Sospedra, A. Moreira, S. Knauth, R. Berkvens, R. Montoliu, O. Belmonte, S. Trilles, M. João Nicolau, F. Meneses, A. Costa, A. Koukofikis, M. Weyn, and H. Peremans, "A realistic evaluation of indoor position-

ing systems based on Wi-Fi fingerprinting: The 2015 EvAALETRI competition," *Journal of Ambient Intelligence and Smart Environments*, vol. 9, no. 2, pp. 263–279, feb 2017.

[12] E. García, P. Poudereux, Á. Hernández, J. J. García, and J. Ureña, "DS-UWB indoor positioning system implementation based on FPGAs," *Sensors and Actuators A: Physical*, vol. 201, pp. 172–181, oct 2013.

[13] M. Weyn, G. Ergeerts, R. Berkvens, B. Wojciechowski, and Y. Tabakov, "DASH7 Alliance Protocol 1.0: Low-Power, Mid-Range Sensor and Actuator Communication," in *2015 IEEE Conference on Standards for Communications and Networking (CSCN)*. Tokyo, Japan: IEEE, 2015, pp. 1–6.

[14] R. Berkvens, B. Bellekens, and M. Weyn, "Signal Strength Indoor Localization using a Single DASH7 Message," in *Indoor Positioning and Indoor Navigation (IPIN), 2017 International Conference on*. Sapporo, Japan: IEEE, 2017, pp. 1–7.

[15] B. Praats, R. Berkvens, G. Ergeerts, and M. Weyn, "Large Scale Distributed Localization Based on RSS and Mass-Spring Model," in *10th International Conference on P2P, Parallel, Grid, Cloud and Internet Computing (3PGCIC)*. Krakow, Poland: IEEE, 2015, pp. 1–6.

[16] IDLab, "OSS-7," 2018. [Online]. Available: http://mosaic-lopow.github.io/dash7-ap-open-source-stack/

[17] F. Letourneux, S. Guivarch, and Y. Lostanlen, "Propagation models for Heterogeneous Networks," in *Antennas and Propagation (EuCAP), 2013 7th European Conference on*. Gothenburg, Sweden: IEEE, 2013, pp. 3993–3997.

[18] O. W. Ata, A. M. Shahateet, M. I. Jawadeh, and A. I. Amro, "An Indoor Propagation Model Based on a Novel Multi Wall Attenuation Loss Formula at Frequencies 900 MHz and 2.4 GHz," *Wireless Personal Communications*, vol. 69, no. 1, pp. 23–36, mar 2013.

[19] B. Bellekens, R. Penne, and M. Weyn, "Validation of an indoor ray launching RF propagation model," in *2016 IEEE-APS Topical Conference on Antennas and Propagation in Wireless Communications (APWC)*. IEEE, sep 2016, pp. 74–77.